Cell Search in W-CDMA

Yi-Pin Eric Wang, *Member, IEEE,* and Tony Ottosson, *Member, IEEE*

***Abstract*—In a CDMA cellular system, the process of the mobile station searching for a cell and achieving code and time synchronization to its downlink scrambling code is referred to as cell search. Cell search is performed in three scenarios: initial cell search when a mobile station is switched on, idle mode search when inactive, and active mode search during a call. The latter two are also called target cell search. This paper presents algorithms and results for both initial and target cell search scenarios for the Wideband CDMA (W-CDMA) standard. In W-CDMA, the cell search itself is divided into five acquisition stages: slot synchronization, frame synchronization and scrambling code group identification, scrambling code identification, frequency acquisition, and cell identification. Initial cell search needs all five stages, while target cell search in general does not need the last two stages.**

A pipelined process of the first three stages that minimizes the average code and time acquisition time, while keeping the complexity at a reasonable level, is considered. The frequency error in initial cell search, which may be as large as 20 kHz, is taken care of by partial symbol despreading and noncoherent combining. Optimization of key system parameters such as the loading factors for Primary Synchronization Channel, Synchronization Channel, and Common Pilot Channel for achieving the smallest average code and time acquisition time is studied. After code and time synchronization (the first three stages), a maximum likelihood (ML)-based frequency acquisition method is used to bring down the frequency error to about 200 Hz. The gain of this method is more than 10 dB compared to an alternative scheme that obtains a frequency error estimate using differential detection.

***Index Terms*—Acquisition, cell search, code division multiple access, frequency error estimation, spread spectrum communication, synchronization.**

I. Introduction

THIRD-GENERATION (3G) cellular systems are currently being standardized in various standardization bodies. The main objectives are to provide higher data rate services with improved service quality and capacity compared to the second-generation cellular systems. Among the 3G cellular systems being considered, IS-2000 [1] (in North America) and Wideband Code-Division-Multiple-Access (W-CDMA) [1], [2] (in Europe and Japan) are both based on direct-sequence code-division multiple-access (DS-CDMA) technology. In these systems, spreading codes are used to differentiate physical channels from the same transmitter, and scrambling codes are used to differentiate transmitters. A mobile station (MS) needs to code and time synchronize to the scrambling code used by the serving cell before any communications with the base station can take place. One of the major differences between W-CDMA and IS-2000 is that W-CDMA supports asynchronous base stations, whereas IS-2000 relies on synchronized base stations. With synchronized base stations, all cells (or sectors) can use shifts of the same scrambling code, so that a cell is identified by a unique code phase shift of the scrambling code. On the other hand, without time and frequency synchronization between base stations, using different phases of the same code for scrambling is not sufficient to resolve the code ambiguity in the presence of time ambiguity. Thus, in an asynchronous CDMA system, cells can only be identified by using distinct scrambling codes. W-CDMA uses 512 downlink primary scrambling codes, allowing unique cell identification in every cluster of 512 cells [3]. The process of searching for a cell and synchronizing to its downlink scrambling code is often referred to as cell search. Cell search is necessary after the MS has switched on (initial search), and during idle and active modes, for identifying new camping cells or handover candidates, respectively. Idle and active mode search is also called target cell search. The performance of cell search impacts the perceived switch-on delay (initial search), stand-by time (idle mode search), and link quality (active mode search), and thus is important to MS design.

In addition to code and time uncertainty, the degree of frequency uncertainty can be large during initial search. Mass produced consumer electronics commonly use inexpensive and rather inaccurate crystal oscillators. Such crystal oscillators have inaccuracies in the range of 3–13 ppm, giving rise to a frequency error in the range of 6–26 kHz, when operated at 2 GHz. Such a frequency error, if not corrected, results in severe degradation in receiver performance so that the receiver communication functions fail. An important goal for the MS is thus to reduce its frequency error to a reasonable range during initial search so that further communication functions can take place. Cell search in W-CDMA deals with rather large code, time, and frequency uncertainties, and thus poses an interesting problem for system and MS design.

This paper addresses algorithms for cell search in W-CDMA. Both initial and target cell search scenarios are studied. The frequency errors considered are 20 kHz and 0 Hz, respectively, for the initial cell search and target cell search. Instead of the traditional method sequentially searching through code, time, and frequency [4, pp. 223–225], the proposed method first acquires code and time synchronization assuming a large frequency error, and then performs frequency acquisition. The synchronization process in W-CDMA can thus be viewed as the five stage process of 1) slot synchronization, 2) frame synchronization and scrambling code group identification, 3) scrambling code identification, 4) frequency acquisition, and 5) cell identification. The combined goal of the first three stages is to deliver a reliable code- and time-candidate to the frequency acquisition stage (stage 4) with low delay and low complexity. To minimize the delay, we consider a pipelined

Manuscript received August 1999; revised February 28, 2000.

Y.-P. E. Wang is with Ericsson Inc., RTP, NC 27709 USA (e-mail: wang@rtp.ericsson.se).

T. Ottosson is with the Department of Signals and Systems, Chalmers University of Technology, SE-412 96 Göteborg, Sweden (e-mail: tony.ottosson@s2.chalmers.se).

Publisher Item Identifier S 0733-8716(00)06114-X.

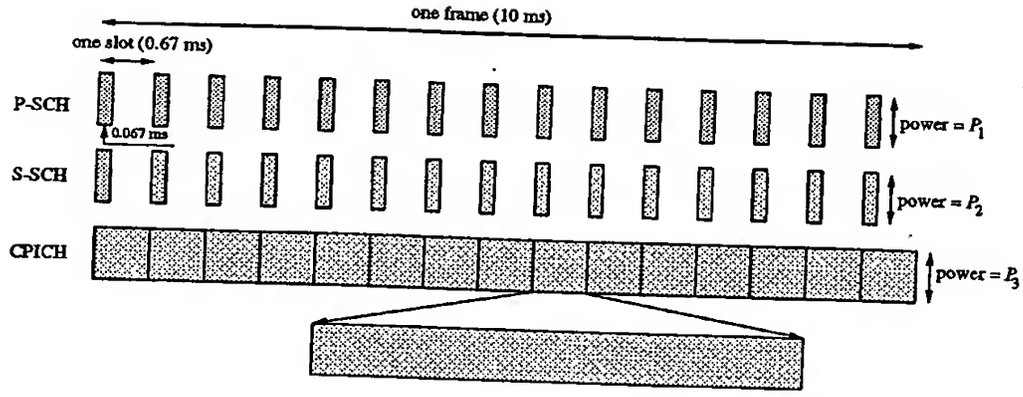

Fig. 1. Frame and slot structures for CPICH, P-SCH, and S-SCH.

process of these first three stages with all stages continuously running to produce results for the next stage. The effect of the large frequency error in these stages is reduced using partial symbol despreading with noncoherent combining. In addition, the possibility of using coherent accumulation in stage 2 (frame synchronization and scrambling code group identification) is exploited. We will show that using coherent accumulation in stage 2 significantly improves cell search performance. We will also show that such a coherent detection scheme is robust even when the channel estimation is severely degraded by an interfering synchronization signal. For scrambling code identification, we introduce a low complexity method consisting of symbol-by-symbol detection of the most likely scrambling code and then majority voting of the most likely scrambling code over one or several frames. An advantage with this proposed method is that the threshold needed in the majority voting can be determined analytically for a target false detection probability. The average acquisition time for code and time synchronization is used to optimize the system and MS design parameters. We will show that by optimizing these parameters, the acquisition time can be reduced significantly. Once a highly reliable code and time candidate is found, the frequency error is estimated using a maximum-likelihood based low-complexity method.

The paper is organized as follows. Section II describes synchronization channels and cell search procedures in W-CDMA. In Section III, the system and signal models are given. Code and time acquisition is studied in Section IV. The issue of parameter optimization for achieving the best average acquisition time is addressed in Section V. In Section VI, frequency acquisition is investigated. Finally, conclusions are given in Section VII.

II. Synchronization Channels and Cell Search Procedure

In W-CDMA, a cell is identified mainly by its downlink scrambling code. There are 512 primary downlink scrambling codes reused throughout a system. These 512 codes are based on length $2^{18} - 1$ Gold sequences truncated to one frame interval, which is 38 400 chips for the chip rate 3.84 Mchips/s. To reduce the complexity of searching through the 512 downlink primary scrambling codes, the concept of code grouping and the use of code group indicator codes (GIC) were introduced in [5] and [6]. The scrambling code is identified by first identifying its code group to significantly reduce the degree of code uncertainty. The complexity of cell search is further reduced by combining code group identification and frame boundary synchronization into one stage [7]. With this scheme, the time uncertainty is completely resolved when the code group identity is obtained. As a result, the complexity of identifying the scrambling code in the identified code group is significantly reduced. Schemes with further complexity reduction by increasing the number of code groups were proposed in [8]. According to [3], the 512 downlink primary scrambling codes are divided into 64 groups, each of 8 codes.

To facilitate cell search, three channels are used, namely the Primary Synchronization Channel (P-SCH), the Secondary Synchronization Channel (S-SCH), and the Common Pilot Channel (CPICH) [9]. The P-SCH together with the S-SCH are also referred to as the Synchronization Channel (SCH). Fig. 1 illustrates the slot and frame formats of these channels. Each frame of 38 400 chips (or 10 ms) is divided into 15 slots, of each 2560 chips (or 0.67 ms). Observe that both P-SCH and S-SCH have a 10% duty factor.

The CPICH, which is used to carry the downlink common pilot symbols, is scrambled by the primary downlink scrambling code of the cell. Within each CPICH time slot, there are 10 pilot symbols, each spread by 256 chips. All symbols are QPSK modulated, and the modulation values of the pilot symbols are known once the MS knows the frame boundary. The spreading sequence of CPICH is taken from the set of Orthogonal Variable Spreading Factor (OVSF) codes [3], maintaining mutual orthogonality between CPICH and the other downlink channels also spread by OVSF codes.

Unlike CPICH, neither the P-SCH nor the S-SCH is scrambled by the primary downlink scrambling code. Instead of the OVSF codes, other sequences of length 256 chips are used. The P-SCH sequence is transmitted once in the same position in every slot, and can thus be used for detecting the slot boundary. Furthermore, all cells use the same P-SCH sequence. As a result, only one P-SCH matched filter is needed to detect the slot boundaries of downlink signals. To reduce the complexity of the P-SCH matched filter, the P-SCH sequence is derived from the

Kronecker product of two sequences of length 16 [10]. With this property, the P-SCH matched filter can be implemented as two concatenated matched filters, each matched to one of the two constituent length 16 sequences, achieving a complexity reduction by approximately a factor of 8.

The S-SCH is used to identify the frame boundary and scrambling code group identity. Unlike the P-SCH sequence, the S-SCH sequences vary from slot to slot. There are 16 S-SCH sequences, mapped correspondingly to 16 S-SCH symbols, labeled from 1–16. A frame (15 slots) of 15 such S-SCH symbols forms a codeword taken from a codebook of 64 codewords. The same codeword is repeated every frame in a cell. These 64 codewords correspond to the 64 code groups used throughout the system; thus a code group can be detected by identifying the codeword transmitted in every S-SCH frame. Furthermore, the 64 codewords are all chosen to have distinct code phase shifts, and any phase shift of a codeword is different from all phase shifts of all other codewords. With these properties, the frame boundary can be detected by identifying the correct starting phase of the S-SCH symbol sequence. To maximize the minimum symbol distance of the codebook, between different cyclic shifts of the same codeword or between any cyclic shifts of different codewords, the use of a Comma-Free Reed–Solomon (RS) code was proposed [11]. For 15 slots per frame, a (15, 3) Reed–Solomon (RS) code over GF(16) is used. The RS code has a minimum distance of 13. Moreover, to minimize cross-channel interference, the 16 S-SCH sequences and the P-SCH are mutually orthogonal [3].

Given the above Synchronization Channels and CPICH, code and time synchronization can be achieved by the following stages [12]: 1) slot boundary detection based on P-SCH (using a P-SCH matched filter); 2) frame boundary detection and scrambling code group identification based on S-SCH (using correlators, correlating against 16 S-SCH sequences, and an RS decoder); 3) scrambling code detection based on CPICH (using correlators, correlating against all scrambling codes in the identified code group). For initial search, the ultimate goal is to decode the cell identity of the acquired signal. To achieve this, two extra stages are needed: 4) frequency acquisition based on CPICH (to reduce initial frequency error so that the MS can decode the broadcast information); and 5) detecting cell identity (by reading the broadcast information). The frequency acquisition step is necessary because of the large frequency error after MS powered on. Without correcting the frequency error, the cell identity, transmitted in the Broadcast Channel, cannot be decoded reliably. For the target cell search, there is no ambiguity in the mapping from a downlink scrambling codes and the cell identity of a neighboring cell. Thus, identifying (and synchronizing to) the downlink scrambling code is sufficient to identify any given cell of interest.

We will focus on the code, time, and frequency acquisition aspects of cell search. Hence, stage 5 will not be addressed. Pipelined processing for stages 1, 2, and 3 is considered, as illustrated in Fig. 2. Stage 4—frequency acquisition—is only activated when time and code synchronization is achieved. To minimize the delay in the pipe (no idle time in the pipe), the synchronization times used in stages 1, 2, and 3 are the same (N_t slots). According to Fig. 2, stage 1 always generates a list of slot

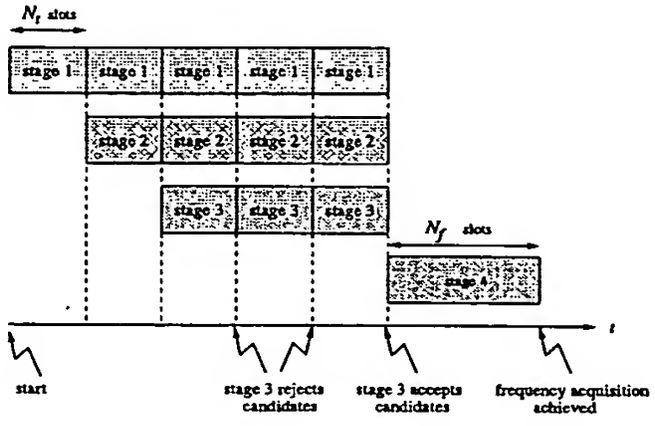

Fig. 2. Cell search procedures.

boundary candidates at the end of each cycle. Based on each of the slot boundaries detected in stage 1, stage 2 finds S-SCH and performs S-SCH correlations and RS decoding. At the end of each detection cycle, stage 2 always gives a list of candidates of frame boundary-code group pair to stage 3 for identification of the scrambling code. In contrast to stages 1 and 2, stage 3 only activates stage 4, when a candidate is detected with high confidence. The acquisition time for code and time synchronization is of interest. According to Fig. 2, the acquisition time can be defined as the time interval between the time when the pipelined process started and the time when stage 3 terminates the process. If stage 3 went through K_3 cycles before it accepts a detected code and terminates the pipelined process, the acquisition time can be given by

$$T_{\text{acq}} = (K_3 + 2)N_t T_{\text{slot}} \tag{1}$$

where T_{slot} is the slot duration.

III. System and Signal Model

In this section, we describe system and signal models. First, to evaluate the performance of each of the individual cell search stages, a signal model as illustrated in Fig. 3 is used. The unity-power desired signal $s_d(t)$ is scaled with power P_d and the unity-variance complex Gaussian noise $n(t)$ is scaled by power P_X. Hence, the signal-to-noise ratio (SNR) is given by P_d/P_X. For stages 1 and 2, the desired signal is the Synchronization Channel (P-SCH + S-SCH); whereas for stages 3 and 4, the desired signal is CPICH.

The term $e^{j2\pi f_e t+\theta}$ in Fig. 3 is used to model the effect of a frequency error f_e, with the phase θ uniformly distributed on $[0, 2\pi]$. The desired signal is passed through a time-varying frequency-selective fading channel with impulse response $g(\tau; t)$, before the impairment component $n(t)$ is added. The impulse response of the fading channel is given by

$$g(\tau; t) = \sum_{l=0}^{L-1} g_l(t)\delta(\tau - \tilde{\tau}_l(t)) \tag{2}$$

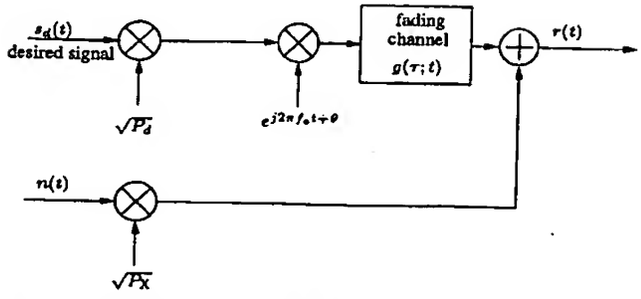

Fig. 3. The signal model used for evaluating the performance of each of the individual cell search stages.

where

L is the number of resolvable multipaths,

$g_l(t)$ is the complex gain of the lth path at time t, and

$\tau_l(t)$ is the delay of the lth path at time t.

Since the delays of multipaths vary slowly with time, they are considered constant in this paper, i.e., $\tau_l(t) = \tau_l$.

For evaluating the performance of the pipelined process shown in Fig. 2, a system model which includes the SCH and CPICH signals as illustrated in Fig. 4 is used. Signals $s_1(t)$, $s_2(t)$, and $s_3(t)$ represent the normalized P-SCH, S-SCH, and CPICH signals; respectively. These signals are later scaled accordingly to have powers of P_1, P_2, and P_3, respectively. Noise $n_1(t)$ is used to model the intra-cell interference, which has total power P_I. This intra-cell interference in our simulations is generated by summing up 16 different equal-power physical channels, each with spreading factor 64. The spreading codes of these interfering channels are chosen to be orthogonal to the one used in CPICH. As a result, in flat fading $n_1(t)$ is orthogonal to the CPICH signal, $s_3(t)$, after despreading. A complex Gaussian process $n_2(t)$ is used to model inter-cell interference. Both $n_1(t)$ and $n_2(t)$ have a variance equal to 1. The frequency error term $e^{j2\pi f_e t+\theta}$ and the impulse response of the fading channel $g(\tau;\, t)$ are the same as those used in Fig. 3.

Instead of giving the absolute powers of all downlink channels, it is often convenient to introduce some power ratios or loading factors of these channels; e.g., the P-SCH loading factor is defined as the power ratio between the P-SCH and the SCH, $\alpha \triangleq P_1/(P_1 + P_2)$. The power ratio between the SCH and all downlink signals from the same cell is defined as $\beta \triangleq (P_1 + P_2)/(P_1 + P_2 + P_3 + P_I)$, and is often referred to as the SCH loading factor. Similarly, the CPICH loading factor is defined as $\gamma \triangleq P_3/(P_1 + P_2 + P_3 + P_I)$. System parameters α, β, and γ are critical to cell search performance. Finally, a geometry factor is defined as the ratio between the power of the desired base station's signal and the postchannel interference, i.e., $G \triangleq (P_1 + P_2 + P_3 + P_I)/P_X$. A larger value of G indicates that the MS is closer to the center of a cell. Typical values for G are in the range of -6 to 6 dB.

Finally, throughout the paper, the P-SCH sequence is represented by $(c_0^{(0)}, c_1^{(0)}, \ldots, c_{255}^{(0)})$, and the mth S-SCH sequence is denoted by $(c_0^{(m)}, c_1^{(m)}, \ldots, c_{255}^{(m)})$, $m = 1, 2, \ldots, 16$, where $c_l^{(m)} \in \{1, -1\}$, $l = 0, 1, \ldots, 255$, $m = 0, 1, \ldots, 16$, are the chip values.

IV. Algorithms for Code and Time Acquisition

In this section, we study the code and time synchronization aspects of cell search. It is assumed that frequency synchronization is not started until code and time synchronization has been achieved (see Fig. 2). Thus, during initial cell search, code and time synchronization has to be achieved in the presence of a rather large frequency error. We will consider both a best-case scenario—a 0 Hz error—and a worst case scenario—a 20 kHz error. The best case scenario is close to a practical operation condition in idle and active modes (target cell search), where a very small frequency error, typically less than 200 Hz, has to be maintained.

A. Stage 1: Slot Synchronization

In stage 1, the P-SCH matched filter is used to detect the slot boundary. Due to a low operating signal-to-noise ratio, the matched filter outputs have to be noncoherently accumulated over many slots to get reliable decision statistics. After accumulation, a number of candidates are identified as possible slot boundary candidates. The receiver block diagram for stage 1 is shown in Fig. 5. In our study, we use one sample per chip for r_k, and optimum sampling timing.

The matched filter output is given by

$$y_k = \sum_{l=0}^{255} r_{k-l} c_{255-l}^{(0)} \tag{3}$$

where, by referring to Fig. 3, the received signal with the P-SCH sequence present is

$$r_k = \sqrt{\alpha P_d} \sum_{l=0}^{L-1} g_{l,k} c_k^{(0)} e^{j2\pi f_e (kT_c - \tau_l) + \theta} + n_k. \tag{4}$$

Here α is the P-SCH loading factor defined in Section III, T_c denotes the chip duration, $g_{l,k} = g_l(kT_c)$, and n_k includes samples of all the interference terms, i.e., S-SCH and $n(t)$. When the frequency error is as large as 20 kHz, using (3) would result in large coherence loss. This is because the exponential component in (4) results in phase rotation in r_k. To alleviate this problem, the P-SCH sequence can be treated as a concatenation of a few short sequences. The P-SCH matched filter therefore consists of filters, each matched to each of the short sequences. The outputs of the short sequence matched filter are combined noncoherently to prevent phase rotations from propagating across different short sequences matched filters. Fig. 6 illustrates such a matched filter architecture.

The matched filter output according to this architecture is given by

$$y_k = \sum_{i=0}^{K-1} \left| y_k^{(i)} \right| \tag{5}$$

$$y_k^{(i)} = \sum_{l=0}^{M-1} r_{k-iM-l} c_{255-iM-l}^{(0)} \tag{6}$$

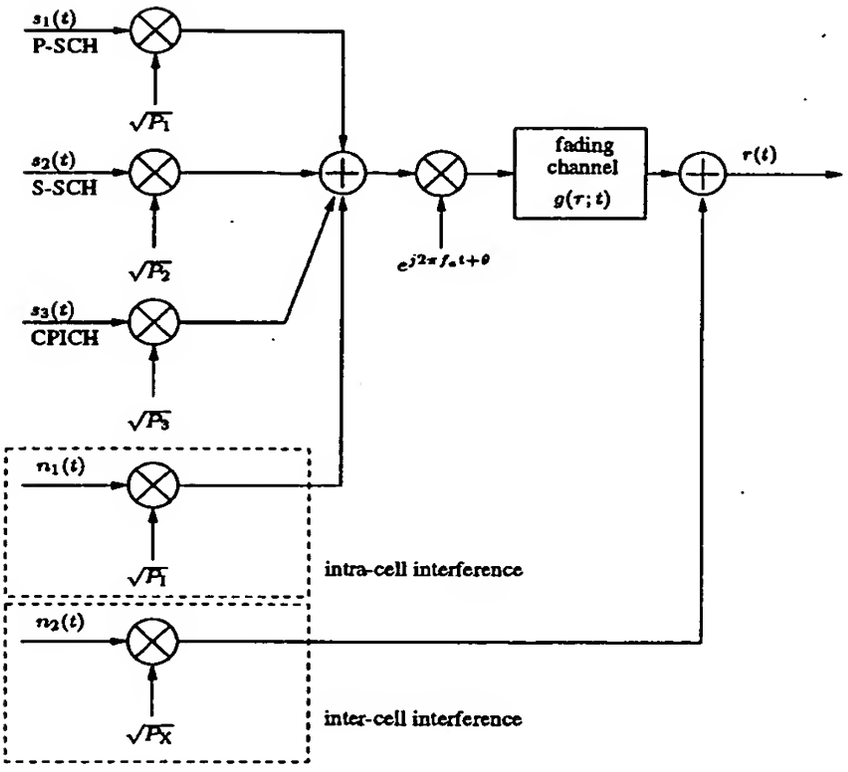

Fig. 4. The signal model used for evaluating the performance of the pipelined cell search process.

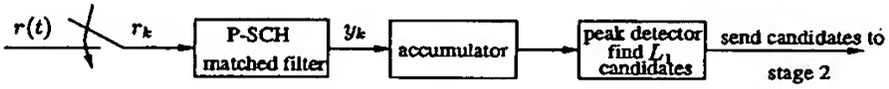

Fig. 5. Slot boundary detector.

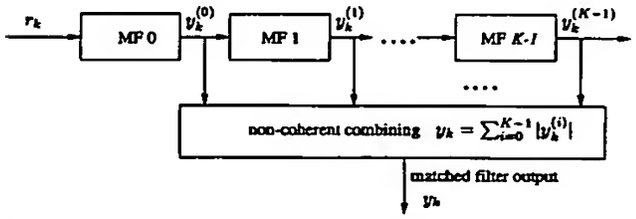

Fig. 6. P-SCH matched filter for handling large frequency errors.

where M is the length of each short sequence, and K is the number of short sequences such that $KM = 256$. The length of each short sequence, M, determines the performance of slot synchronization in the presence of frequency error. A larger M results in more phase rotation during matched filtering and larger incoherence loss. However, a large M also results in better noise suppression and may thus improve performance. Therefore, M has to be optimized for different frequency errors. In [13], it was shown that the signal-to-noise ratio (SNR) for the peak of matched filter output is

$$\mathrm{SNR}(M) = \frac{1}{P_N} \cdot \frac{\sin^2(\pi f_e M T_c)}{M \sin^2(\pi f_e T_c)} \tag{7}$$

where P_N is the power of the noise. For initial cell search, with a frequency error of 20 kHz, $M = 64$ is the best choice, assuming that M is restricted to a power of 2. For target cell search, with a frequency error typically less than 200 Hz, the best choice is $M = 256$. In the following, we use $M = 64$ for the initial cell search and $M = 256$ for the target cell search.

The performance of stage 1 with 15 slots (10 ms) synchronization time in flat fading channels is shown in Fig. 7. Slot synchronization error rate, defined as the probability that none of the detected candidates coincides with the slot boundary of any resolvable multipath, is plotted versus SNR. Referring to Fig. 3, SNR $= P_d/P_X$. Note that P_d includes the power from both the P-SCH and the S-SCH. Furthermore, the results in Fig. 7 are based on $\alpha = 0.5$, i.e., the power of Synchronization Channel is evenly split between P-SCH and S-SCH and that only one candidate is detected ($L_1 = 1$). If stage 1 gives more than one candidate to stage 2, the performance improves, at the expense of higher stage 2 complexity. From Fig. 7, we conclude that 20 kHz frequency error (initial search) results in significant loss in stage 1 performance, and that the performance improves with increasing fading rate. A higher fading rate gives rise to faster received level variation, and thus less time correlation between fading channel realizations. When there is less time correlation

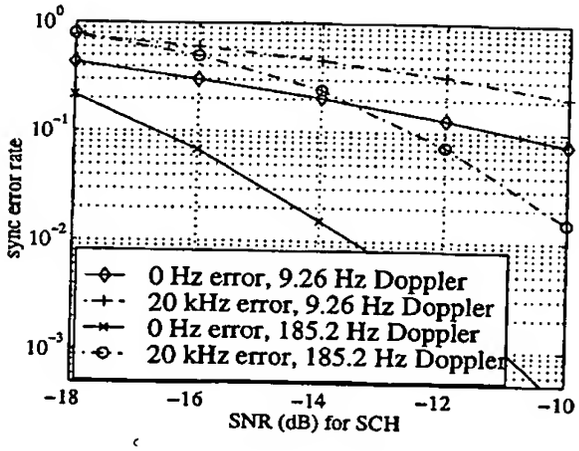

Fig. 7. Stage 1 performance ($N_t = 15$, $\alpha = 0.5$, flat fading).

between fading channel realizations, better time diversity gain can be achieved when accumulating the matched filter output over more than one slot.

B. Stage 2: Frame Synchronization and Code Group Identification

After achieving slot synchronization, S-SCH can be easily found. In stage 2, the receiver operations start with correlating the received signal of SCH with all 16 S-SCH sequences, and then accumulates S-SCH correlations over N_t slots according to the 64 RS codewords used, each with 15 hypothesized frame boundaries. The total number of hypotheses is therefore 960 (64 codewords times 15 shifts). At the end, the hypothesis with the largest accumulated metric is chosen as the candidate for frame boundary-code group pair, which is given to stage 3 for scrambling code identification. Due to the frequency error and fading, there is a considerable amount of phase rotation in one slot duration. Thus, noncoherent accumulation has to be used for combining S-SCH correlations from slot to slot, if such a phase rotation is not corrected. However, since P-SCH is always transmitted along with S-SCH, the P-SCH correlation can be used as a phase reference to phase-correct the S-SCH correlations. We address both noncoherent and coherent detection below.

1) Noncoherent Detection: Let $r_j^{(k)}$ be the jth sample of the kth received SCH symbol, where $j = 0, 1, 2, \ldots, 255$ (i.e., for each slot there are 256 samples), and $k = 0, 1, \ldots, N_t - 1$. Furthermore, let $w_k(j)$ be the jth symbol of the RS codeword associated with code group k, $k = 1, 2, \ldots, 64$, and $j = 0, 1, \ldots, 14$. Symbol $w_k(j)$ takes values in $\{1, 2, \ldots, 16\}$, with each symbol value mapped onto an S-SCH sequence. The algorithm for stage 2 consists of the following steps.

i) For received slot k, calculate S-SCH correlations

$$S_m(k) = \left| \sum_{j=0}^{255} r_j^{(k)} c_j^{(m)} \right|, \qquad m = 1, 2, \ldots, 16, \quad k = 0, 1, \ldots, N_t - 1. \tag{8}$$

Note that there are $16N_t$ correlations in total. The summation in (8) assumes that the frequency error during this stage is small so that coherent combining over 256 chips is possible. As mentioned earlier, for a 20 kHz frequency error, it is better to treat each S-SCH sequence as 4 short sequences, each of 64 chips. Coherent correlation is done on a short sequence, and the correlation values of short sequence are combined noncoherently. For this case, (8) is modified as

$$S_m(k) = \sum_{l=0}^{3} \left| \sum_{j=64l}^{64(l+1)-1} r_j^{(k)} c_j^{(m)} \right|. \tag{9}$$

ii) Accumulate S-SCH correlation values. Since the RS codewords are periodically repeated in every frame, if $N_t > 15$ (i.e., synchronization time is longer than one frame), the correlation values corresponding to the same S-SCH sequence in different frames can be combined.

$$\tilde{S}_m(k) = \sum_{\substack{j=0 \\ (j \bmod 15)=k}}^{N_t-1} S_m(j), \qquad m = 1, \ldots, 16, \quad k = 0, \ldots, 14. \tag{10}$$

iii) RS code decoding. The brute-force approach is to correlate $\tilde{S}_m(k)$ with each RS codeword and with each cyclic shift.

$$X_i(m) = \sum_{k=0}^{14} \tilde{S}_{w_i(k+m \bmod 15)}(k), \qquad m = 0, \ldots, 14, \quad i = 1, \ldots, 64. \tag{11}$$

The metric $X_i(m)$ is associated with the hypothesis of code group i and frame timing m.

iv) Find the maximum $X_i(m)$. The code group number can be found by

$$\hat{i} = \arg \max_i X_i(m) \tag{12}$$

and the slot number corresponding to the first received slot in this stage is

$$\hat{m} = \arg \max_m X_i(m). \tag{13}$$

The pair $(\hat{i}, \hat{m})$ is given to stage 3 for identification of the primary scrambling code.

2) Coherent Detection: For coherent detection, the P-SCH is used for deriving a channel estimate. The channel estimate is used to phase-correct the S-SCH correlations before combining. With this approach, (8) can be modified to be

$$S_m(k) = \mathrm{Re}\{C_0^*(k) C_m(k)\}, \qquad m = 1, \ldots, 16, \; k = 0, \ldots, N_t - 1 \tag{14}$$

where

$$C_l(k) = \sum_{j=0}^{255} r_j^{(k)} c_j^{(l)}. \tag{15}$$

Note that in (14), $C_0(k)$ corresponds to the P-SCH correlation, and $C_m(k)$ corresponds to the correlation with the mth S-SCH

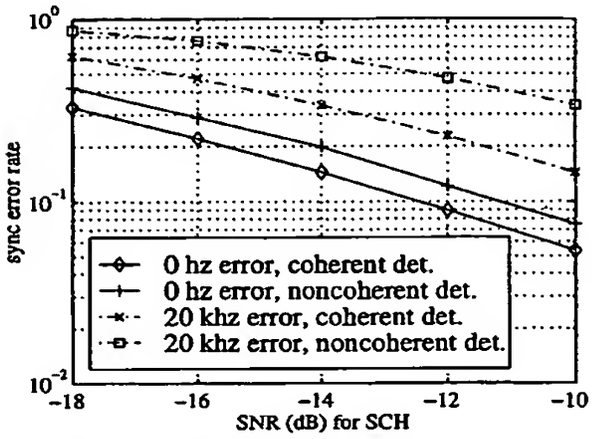

Fig. 8. Stage 2 performance ($N_t = 15$, $\alpha = 0.5$, flat fading, 9.26 Hz Doppler).

sequence. Again, the summation in (15) assumes that the frequency error during this stage is small. If the frequency error is as large as 20 kHz, the following equations can be used instead.

$$S_m(k) = \sum_{l=0}^{3} \mathrm{Re}\left\{C_{0,l}^{*}(k) C_{m,l}(k)\right\} \tag{16}$$

where

$$C_{m,l}(k) = \sum_{j=0}^{63} r_{64l+j}^{(k)} c_{64l+j}^{(m)}. \tag{17}$$

In (16), the partial summation of 64 chips is first phase corrected before added. The remaining steps for coherent detection are the same as those described previously for noncoherent detection.

The performance of stage 2 in a flat fading channel with 9.26 Hz Doppler is shown in Fig. 8, for both coherent and noncoherent detection, and for 0 Hz and 20 kHz frequency errors. Again, the power of Synchronization Channel is evenly split between P-SCH and S-SCH. The synchronization error rate here is defined as the probability of stage 2 failing to detect the right code group number and frame boundary, given the correct slot boundary is provided. From Fig. 8, we see that coherent detection achieves much better performance than noncoherent detection, especially during initial search when the frequency error is large. However, coherent detection relies on the P-SCH correlation to get a phase reference. In W-CDMA, all the cells use the same P-SCH sequence. When the P-SCH of different cells are time-aligned, the channel estimate obtained through P-SCH correlation will not be accurate. This potential problem with coherent detection will be addressed in the next section. Moreover, compared to stage 1 performance, stage 2 performance is much better, when coherent detection is used.

C. Stage 3: Scrambling Code Identification

After identifying the scrambling code group and achieving frame synchronization, the downlink primary scrambling code can be identified by correlating the CPICH with all possible scrambling codes in the identified code group. The number of scrambling codes in the identified code group, N_{LC}, depends on the operating scenario. For initial search, $N_{\mathrm{LC}} = 8$, whereas for idle and active mode search, N_{LC} is typically 1 or 2, given a good system-wide code planning [8]. One of the main design considerations in this stage is the probability of false detection. According to Fig. 2, stage 3 accepts a candidate only when the detection metric is greater than a threshold, where the threshold is predetermined to achieve a certain false detection probability. For initial search, once a scrambling code is "detected," the processes of frequency acquisition (stage 4) and eventually reading the broadcast information (stage 5) are started. For idle and active mode search, a detected scrambling code will be time-tracked and the signal-to-interference ratio (SIR) thereof will be measured and reported back to the base station. To minimize unnecessary MS activities, it is thus desirable to have a very low false detection probability during stage 3.

TABLE I
STAGE 3 DETECTION THRESHOLDS

N_{LC}	8	8	8	8	2	2	2	2
J	150 (10 ms)	150	300 (20 ms)	300	150	150	300	300
P_{FA}	10^{-4}	10^{-3}	10^{-4}	10^{-3}	10^{-4}	10^{-3}	10^{-4}	10^{-3}
D	38	35	64	60	99	95	184	178

The detection scheme considered in this paper is to correlate each received CPICH symbol with N_{LC} hypothesized scrambling codes. The correlation is performed with 256 or 64 chips of coherent combining depending on the frequency error scenario as discussed earlier. For each CPICH symbol, the scrambling code with the largest correlation value is chosen. At the end, after collecting $10N_t$ symbols (i.e., N_t slots with 10 symbols per slot), a majority vote is used to determine the most likely scrambling code. The detected scrambling code is accepted only when the detection metric (number of votes) associated with the detected scrambling code is greater than the predetermined threshold. The number of symbols used in stage 3 is $J = 10N_t$, and let D be the detection threshold. Using the union bound, the false detection (false alarm) probability can be approximated by

$$P_{\mathrm{FA}} = N_{\mathrm{LC}} \sum_{j=D+1}^{J} \binom{J}{j} \left(\frac{1}{N_{\mathrm{LC}}}\right)^{j} \left(\frac{N_{\mathrm{LC}}-1}{N_{\mathrm{LC}}}\right)^{J-j}. \tag{18}$$

According to our study, this union bound is very tight for $P_{\mathrm{FA}} \leq 0.01$. Using (18), the detection threshold D can be determined. Table I lists the values of D in various scenarios.

Fig. 9 shows the performance of stage 3 in a flat fading channel with 9.26 Hz Doppler and 10 ms synchronization time ($N_t = 15$). The target false detection probability is 10^{-4}, and the miss detection probability is defined as the probability of stage 3 failing to detect a scrambling code given it starts with a correct frame boundary and code group number. This occurs when the detection metric is less than the predetermined threshold D. The two curves in Fig. 9 correspond respectively to the initial cell search (dash line) and target cell search (solid line) scenarios.

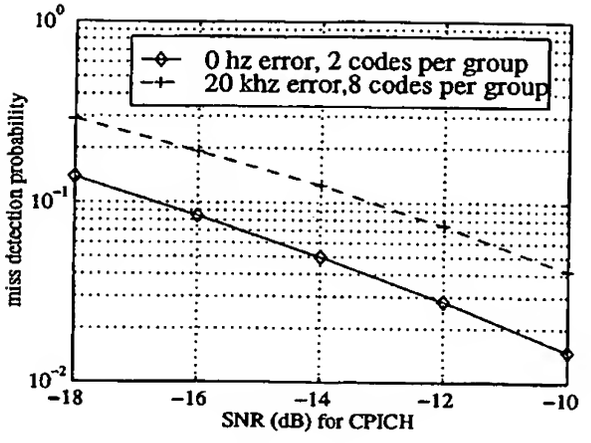

Fig. 9. The performance of stage 3 in a flat fading channel with 9.26 Hz Doppler. The target false detection probability is 10^{-4} and the synchronization time is 10 ms ($N_t = 15$).

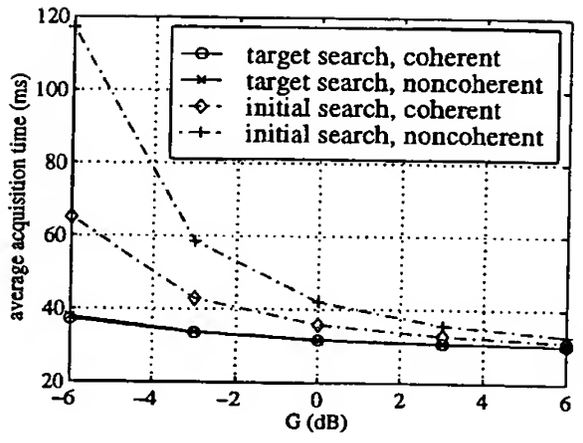

Fig. 10. Average acquisition time in a flat fading channel with 9.26 Hz Doppler ($N_t = 15, \alpha = 0.5, \beta = 0.1, \gamma = 0.1$).

V. Performance of Pipelined Process and Parameter Optimization

In this section, the performance of the three-stage pipelined cell search process illustrated in Fig. 2 is studied. Both initial and target cell search scenarios are considered. For initial search, the MS has to search through all 512 possible primary scrambling codes, and as long as it can identify one valid scrambling code, the search process is considered a success. In target cell search scenarios, we assume that the MS is given a list of target scrambling codes from the serving base station. In our study, we consider that the *target* scrambling codes are distributed among 16 code groups, and each code group can have at most two target scrambling codes. The acquisition time during target search is defined as the time required to identify a desired target code among the list of all target scrambling codes. The algorithm described in Section IV-C is used to determine if a code is identified reliably, with a false detection probability of 10^{-4}.

Fig. 10 shows the average acquisition time in a flat fading channel with 9.26 Hz Doppler. The system design parameters defined in Section III are set to be $(\alpha, \beta, \gamma) = (0.5, 0.1, 0.1)$, and the synchronization time per stage is $N_t = 15$ slots (i.e., 10 ms). It can be seen that during initial search when the MS is at the cell edge (i.e., lower G values), using coherent detection in stage 2 significantly reduces the average acquisition time. The improvement is seen as 15–40% reduction in average acquisition time compared to using noncoherent detection when $-6 \leq G \leq 0$ dB. For target search, the benefit of using coherent detection in stage 2 seems small.

Next we compare the performance of the pipelined process to a serial process similar to the one used in [6]. The serial search process is illustrated in Fig. 11, which has 30 ms synchronization time in stage 1, 20 ms synchronization time in stage 2, and 10 ms synchronization time in stage 3. It can be seen that the pipelined search process considered achieves faster acquisition time (Fig. 12).

As mentioned in Section IV-B, coherent detection in stage 2 needs to obtain a phase reference from the P-SCH correlation. In rare scenarios where two SCH signals are slot-aligned, the phase reference may be deteriorated, and thus may have negative impact on the cell search performance. To study this further, we use a two-cell simulation model. In addition to the signals shown in Fig. 4, another set of signals for a second cell is generated, including a P-SCH, an S-SCH, a CPICH, and an intra-cell interference signal. These signals are of the same power as their counterparts in the first cell. Signals of the same cell are faded together just as illustrated in Fig. 4, whereas signals of different cells are faded independently. Fig. 13 shows the average acquisition time for initial search in the slot-aligned scenario. For comparison, the performance when the two SCH signals are not slot-aligned is also shown. The system and receiver parameter setting is the same as those used in Fig. 10, and the variable G' is defined as the ratio between the total power of the first cell and $P_{\mathcal{X}}$. Since the two cells have the same total transmitted power, the geometry factor of each of the cells can be related to G' by $G = 1/(1 + (G')^{-1})$. From Fig. 13, it is found that using coherent detection in stage 2 maintains its performance advantage over noncoherent detection, even when the two SCH signals are slot-aligned.

To study the average acquisition time in realistic channel conditions, three W-CDMA test channels—CASE I (Indoor, 3 km/h), CASE II (Indoor to Outdoor and Pedestrian, 3 km/h), and CASE III (Vehicular, 120 km/h) [14]—are used. Table II lists the multipath delay profile of these test channels. The average acquisition time for initial search is shown in Fig. 14. For comparison purposes, the performance in a flat fading channel with 9.26 Hz Doppler is also shown. It is found that for initial search, the CASE III channel requires the longest acquisition time. This is because the large frequency error during initial search results in significant signal loss; and in a highly dispersive channel such as the CASE III channel, the energy of each resolvable multipath becomes extremely weak. Although CASE III has better path diversity (more resolvable multipaths) and time diversity (higher vehicular speed), the performance is essentially limited by the weak signal strength of each multipath. However, from Fig. 14, it can be seen that when the mobile is closer to the center of a cell (larger geometry factor G

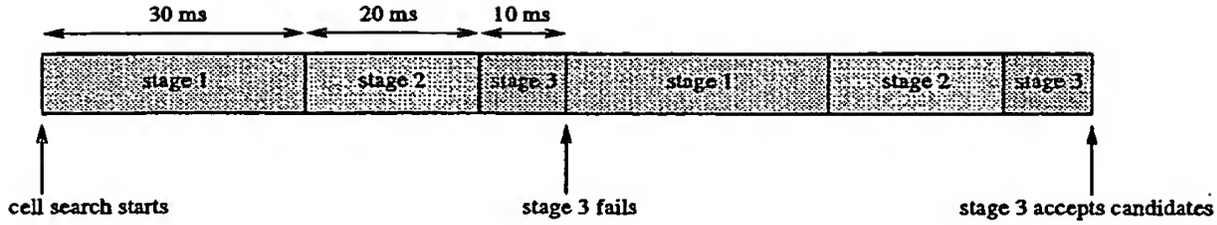

Fig. 11. A serial search process with 30 ms synchronization time in stage 1, 20 ms synchronization time in stage 2, and 10 ms synchronization time in stage 3.

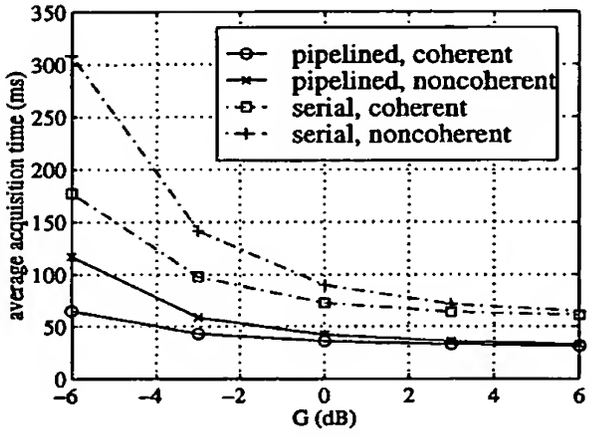

Fig. 12. Average acquisition time for initial search in a flat fading channel (9.26 Hz Doppler), pipelined versus serial search ($\alpha = 0.5, \beta = 0.1, \gamma = 0.1$, 20 kHz frequency error).

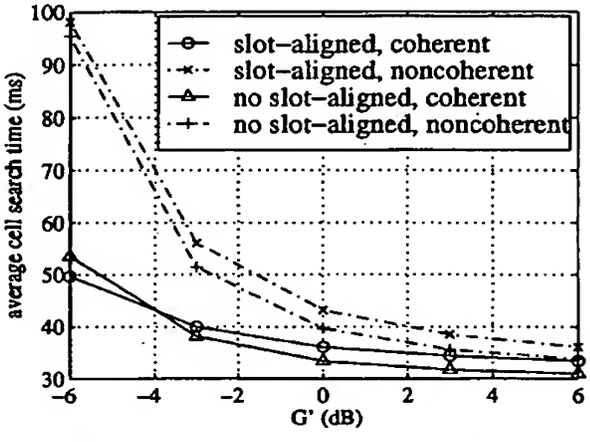

Fig. 13. Average acquisition time for initial search in a flat fading channel (9.26 Hz Doppler), slot-aligned versus no slot-alignment ($N_t = 15, \alpha = 0.5$, $\beta = 0.1, \gamma = 0.1$, 20 kHz frequency error).

and stronger desired signal), the performance in the CASE III channel is very close to the other test channels. This is because as the signal strength of each multipath becomes stronger, path and time diversity becomes more helpful. Moreover, for $G > -3$ dB, the average acquisition time during initial search is less than 100 ms in all W-CDMA test channels.

The performance of target search is shown in Fig. 15. It can be seen that a target can be identified within 42 ms in all test channels of interest, given its geometry factor is greater than -6

TABLE II
DELAY PROFILES W-CDMA TEST CHANNELS

CASE I (3 km/h)		CASE II (3 km/h)		CASE III (120 km/h)	
relative delay	relative average power	relative delay	relative average power	relative delay	relative average power
0 ns	0 dB	0 ns	0 dB	0 ns	0 dB
976 ns	-10 dB	976 ns	0 dB	260 ns	-3 dB
		20000 ns	0 dB	521 ns	-6 dB
				781 ns	-9 dB

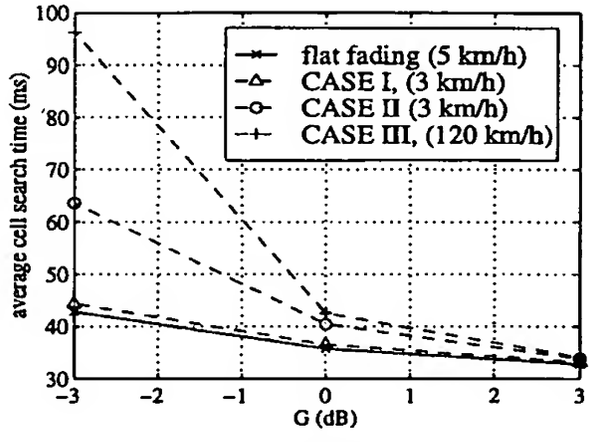

Fig. 14. Average acquisition time for initial search in various W-CDMA test channels ($N_t = 15, \alpha = 0.5, \beta = 0.1, \gamma = 0.1$, 20 kHz frequency error).

dB. Similar to the case of initial search, path and time diversity helps when the desired signal is strong; and when the desired signal is weak, higher dispersiveness results in weaker signal energy per multipath, which limits the performance.

An interesting optimization problem for the Synchronization Channel is the power ratio, α, between the P-SCH and the Synchronization Channel. Table III shows the average acquisition time in the CASE III test channel for initial and target search, respectively. The geometry factor is fixed as $G = -3$ dB, and coherent detection is used in stage 2 in both cases. From these results, we conclude that a good choice of α is approximately 0.6–0.7 for the pipelined process considered. This is because stage 2 performance is much better than stage 1 performance. Thus, it is advantageous to increase the power allocation for P-SCH. However, it should be noted that for other cell search processes such as the serial search process shown in Fig. 11, which has different averaging time among the different

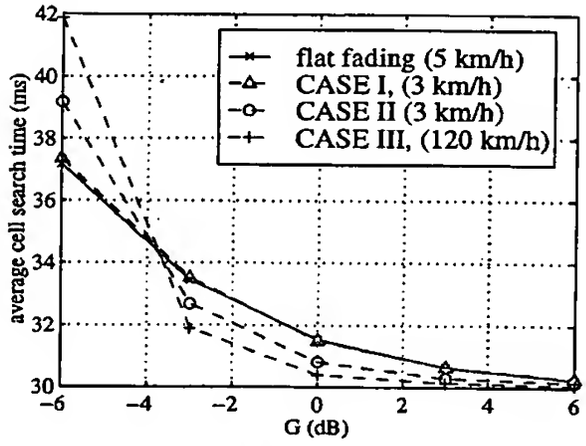

Fig. 15. Average acquisition time for target search in various W-CDMA test channels ($N_t = 15, \alpha = 0.5, \beta = 0.1, \gamma = 0.1$, no frequency error).

TABLE III
AVERAGE ACQUISITION TIME VERSUS THE P-SCH LOADING FACTOR α (CASE III TEST CHANNEL, $G = -3$, $N_t = 15, \beta = 0.1, \gamma = 0.1$)

α	initial search	target search
0.5	96.27 ms	31.90 ms
0.55	82.23 ms	31.63 ms
0.6	74.47 ms	31.52 ms
0.65	69.63 ms	31.59 ms
0.7	67.18 ms	31.83 ms
0.75	68.41 ms	32.25 ms

stages, the best choice of α might be different. Nevertheless, the pipelined process considered is shown to be superior to the serial search process; therefore, to achieve the fastest acquisition time, the system should optimize the parameter setting for the pipelined process.

The CPICH loading factor (γ) and the SCH loading factor (β) are also critical to cell search performance. Higher values of γ and β result in faster acquisition, at the expense of higher interference to other physical channels in the same cell. On the other hand, the system can enhance the in-cell capacity by tolerating longer acquisition time. Table IV shows the average acquisition time as a function of the CPICH loading factor. It is seen that there is not much performance improvement by increasing the CPICH loading factor beyond 10%. However, when the CPICH loading factor is less than 5%, there is significant penalty in the cell search performance. Since in W-CDMA CPICH could also be used for channel estimation, it should be noted that when deciding the CPICH loading factor, the performance of channel estimation also needs to be taken into account. Table V shows the acquisition time as a function of the SCH loading factor. It is seen that when the SCH loading factor is below 10%, there is severe degradation in cell search performance. Since SCH has a duty factor of 10%, effectively it only uses $\beta/10$ total transmitted power of a cell on the average. Thus, lowering β below 10% does not seem to be an attractive system design choice.

TABLE IV
AVERAGE ACQUISITION TIME VERSUS THE CPICH LOADING FACTOR γ (CASE III TEST CHANNELS, $N_t = 15, \alpha = 0.5, \beta = 0.1, G = -3$ dB)

γ	initial search	target search
12.5%	96.15 ms	31.74 ms
10%	96.27 ms	31.90 ms
7.5%	108.13 ms	32.18 ms
5%	155.79 ms	33.29 ms
2.5%	1462.5 ms	44.61 ms

TABLE V
AVERAGE ACQUISITION TIME VERSUS THE SCH LOADING FACTOR β (CASE III TEST CHANNELS, $N_t = 15, \alpha = 0.5, \beta = 0.1, G = -3$ dB

β	initial search	target search
15%	43.35 ms	30.57 ms
12.5%	57.46 ms	30.89 ms
10%	96.27 ms	31.90 ms
7.5%	297.3ms	35.18 ms
5%	2476 ms	52.28 ms

VI. FREQUENCY ACQUISITION (STAGE 4)

In this section, the problem of frequency acquisition is studied. Without loss of generality, we assume that the modulation values for the pilot symbols in CPICH are all 1's. Using the signal model shown in Fig. 3, the CPICH signal can be expressed as

$$s_d(t) = \sum_{i=-\infty}^{\infty} a_i p(t - iT_c) \tag{19}$$

where a_i is the ith chip of the scrambling code, and $p(t)$ is the chip waveform. Similar to (4), the received signal sample can be expressed as (assuming a one-path channel)

$$r_k = \sqrt{P_d} g'_k a_k c^{j(2\pi f_e k T_c + \theta)} + n_k \tag{20}$$

where $g'_k = g_{0,k}$ and τ_0 is set to 0. Although the frequency error detector developed below is based on a one-path channel model, it can be easily extended to cases with dispersive channels.

The first step of frequency acquisition is to despread the CPICH signal as

$$y_i = \sum_{l=0}^{N-1} r_{iN+l} a^*_{iN+l} \tag{21}$$

where N is the despreading factor, and a^* stands for the complex conjugate of a. Assume that $a_k a^*_k = 1$, and the channel coefficient, g'_k, is constant over N chips. It follows that

$$y_i = g'_{iN} e^{j2\pi f_e i N T_c} e^{j\theta} \sum_{l=0}^{N-1} \left\{ e^{j2\pi f_e l T_c} + n_{iN+l} \right\} \tag{22}$$

$$= \tilde{g}_i \left(e^{j\phi(f_e)} \right)^i e^{j\theta'} (A(f_e) + \tilde{n}_i) \tag{23}$$

where $\tilde{g}_i = |g'_{iN}|$, $\phi(f_e) = 2\pi f_e T_d$, $\tilde{n}_i = \sum_{l=0}^{N-1} n_{iN+l}$, and

$$A(f_e) = \sum_{l=0}^{N-1} e^{j2\pi f_e l T_c}. \tag{24}$$

The constant $T_d = NT_c$ is the duration of a despread symbol, and $\tilde{n}_i$ is the white Gaussian component with variance σ^2. Note that the phase of the complex channel coefficient g'_{iN} is folded into the random phase term θ'. Given L_d observables, $\boldsymbol{y} = (y_0, \ldots, y_{L_d-1})$, the log-likelihood function for detecting the frequency error, conditioned on coefficients $\boldsymbol{g} = (\tilde{g}_0, \tilde{g}_1, \ldots, \tilde{g}_{L_d-1})$, is given by [13]

$$\begin{aligned} z_i &\triangleq \ln p(\boldsymbol{y}|f_e = f_i, \boldsymbol{g}) \\ &= \ln I_0\left(\frac{2|A(f_i)|}{\sigma^2} \cdot |Y_i|\right) - \frac{1}{\sigma^2}|A(f_i)|^2 \sum_{l=0}^{L_d-1} |\tilde{g}_l|^2 \end{aligned} \tag{25}$$

where

$$Y_i = \sum_{l=0}^{L_d-1} \tilde{y}_l e^{-j2\pi l f_i T_d} \tag{26}$$

and $\tilde{y}_l = y_l \tilde{g}_l^*$. Note that in (26), Y_i is simply the Discrete Fourier Transform (DFT) of $\tilde{\boldsymbol{y}} = (\tilde{y}_0, \ldots, \tilde{y}_{L_d-1})$ at frequency f_i. Given T_c, N, and f_i, the values of $A(f_i)$ can be precalculated using (24). The ML detector for frequency error f_e is thus finding a hypothesized frequency error f_i which maximizes z_i, within the frequency uncertainty region $[-f_{\max}, f_{\max}]$. The magnitude of the largest possible frequency error, $f_{\max}$, depends on the choice of crystal oscillator.

In practice, one cannot have an infinite number of hypotheses; instead a finite number K_h of hypotheses is used. It is preferred that K_h is a power of 2, because for such K_h, the Fast Fourier Transform (FFT) can be used. However, for a finite K_h, the accuracy of frequency detection is limited by the resolution of FFT. For a despread symbol duration T_d, the frequency resolution is $\Delta f = 1/T_d/K_h$, and the hypothesized frequency error is

$$f_i = \begin{cases} (i-1)\Delta f & 1 \le i \le K_h/2+1 \\ -(K_h - i + 1)\Delta f & K_h/2+1 < i \le K_h. \end{cases}$$

From (25), the decision statistic $\boldsymbol{z} = (z_1, z_2, \ldots, z_{K_h})$ for all K_h hypotheses in AWGN can be expressed as

$$\boldsymbol{z} = \ln I_0\left(\frac{2\mathrm{diag}(\boldsymbol{a}|\boldsymbol{Y}^T|)}{\sigma^2}\right) - \frac{L_d \cdot \mathrm{diag}(\boldsymbol{a}\boldsymbol{a}^T)}{\sigma^2} \tag{27}$$

where $\boldsymbol{a} = (|A(f_0)|, |A(f_1)|, \ldots, |A(f_{K_h})|)^T$, and the column vector $\boldsymbol{Y}$ is the K_h-point FFT of $\tilde{\boldsymbol{y}}$. In (27), if elements in vector $\boldsymbol{a}$ is approximated by $A(f_i) \approx A, \forall i$, a simpler suboptimal detector can be derived:

$$\boldsymbol{z}' = |\boldsymbol{Y}|. \tag{28}$$

This suboptimal detector in AWGN is simply the FFT of the despread values. It was shown in [13] that the suboptimal detector achieves performance almost identical to the ML detector. Furthermore, this suboptimal detector is in fact the same as the ML frequency error estimator for a nonspread signal presented in [15] and [16].

As mentioned earlier, with finite K_d, the accuracy of the K_d-Hypothesis ML detector is limited by the frequency resolution Δf of the FFT algorithm. To improve the accuracy beyond this limitation, the idea of taking the derivatives of the log-likelihood function with respect to f_e was proposed in [16] and [17]. Here we propose another alternative based on performing quadratic interpolation in the frequency domain. This algorithm first finds the largest detection statistic z_J and its corresponding frequency hypothesis f_J, and then determines a quadratic curve $z = v_1 f^2 + v_2 f + v_3$, such that the points (f_{J-1}, z_{J-1}), (f_J, z_J), and (f_{J+1}, z_{J+1}) are on the quadratic curve. It can be shown that the peak of the quadratic curve occurs at frequency (and thus our refined estimate)

$$\hat{f}_e = f_J + \left[\frac{3z_{J-1} - 4z_J + z_{J+1}}{2z_{J-1} - 4z_J + 2z_{J+1}} - 1\right] \Delta f. \tag{29}$$

A. Proposed Scheme

Based on the interpolated K_h-Hypothesis ML detector, the following scheme is proposed for achieving initial frequency acquisition in W-CDMA.

The proposed scheme consists of: 1) despreading the CPICH signal using a despreading factor $N = 64$; 2) collecting $L = 40$ despread values per slot;[1] 3) removing the modulation of these despread values using the knowledge of the pilot symbols; 4) calculating the detection statistics $\boldsymbol{z} = (z_1, z_2, \ldots, z_{64})$ using a 64-point FFT ($K_h = 64$), after zero-padding; 5) accumulating the detection statistics $\boldsymbol{z}$ over N_f slots; and 6) performing quadratic interpolation to find the estimated frequency error $\hat{f}_e$. With a chip rate of 3.84 Mchips/s, the frequency resolution of the 64-point FFT used in this scheme is therefore 937.5 Hz.

For comparison, we also study the performance of a differential detection (DD) scheme. In this approach, the CPICH signal is first despread by also using a despreading factor of 64 chips. After removing the modulation of the pilot symbols, each despread value is multiplied by the complex conjugate of its precedent despread value to get a metric relating to the phase rotation between two successive despread values. The metrics are then accumulated over N_f slots, and at the end, the accumulated metric is converted to the corresponding phase error and frequency error. Such a differential detector based scheme suffers from noise enhancement, especially when the signal-to-noise ratio of the despread value is low, e.g., less than 0 dB.

The simulation results for a flat fading channel are shown in Fig. 16. The synchronization time used is 20 ms ($N_f = 30$) and the maximum frequency error is 20 kHz. Results for both slow fading (9.26 Hz) and fast fading (463 Hz) are shown. The synchronization error rate is defined as the probability that the difference between the estimated frequency error and true frequency error is more than 200 Hz. One can see that the proposed

[1]Since there are 2560 chips in a slot, with a despreading factor of 64, 40 despread values can be obtained.

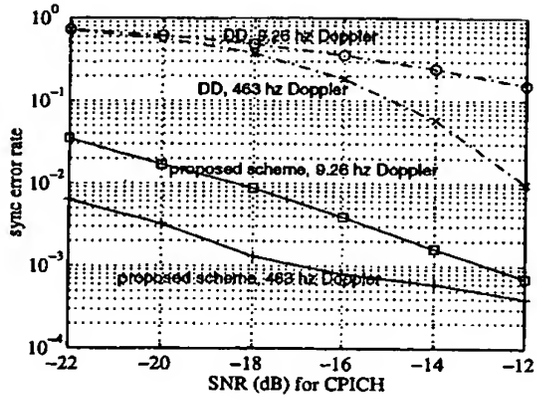

Fig. 16. Performance comparison between the differential detection scheme and the proposed scheme in a flat fading channel. ($N_f = 30$, $f_{max} = 20$ kHz).

scheme outperforms the DD scheme by more than 10 dB. Moreover, the proposed scheme reduces the frequency error from 20 kHz to 200 Hz with a very high reliability. Observe that for the case with 463 Hz Doppler spread, the proposed scheme even achieves frequency accuracy beyond the Doppler spread.

VII. Conclusion

Two scenarios of cell search in Wideband CDMA (W-CDMA) have been studied: 1) the initial cell search when a mobile station is switched on; and 2) the target cell search idle and active modes. The frequency errors considered are 20 kHz and 0 Hz for the initial and target cell search, respectively. The large frequency error results in large incoherence loss during initial search. This problem is solved by partial symbol despreading and noncoherent combining between partial symbols. With a maximum frequency error of 20 kHz, despreading using 64 chips long symbols instead of 256 chips is used. This partial symbol despreading is also used in stage 2 with either noncoherent or coherent combining using the primary synchronization channel to obtain a channel estimate. It is shown that coherent stage 2 detection improves the average acquisition time performance significantly, even in the slot-aligned scenario, where the synchronization channels from two cells are perfectly aligned. Optimization of key system parameters such as Primary Synchronization (P-SCH) Channel, Synchronization Channel (SCH), and Common Pilot Channel (CPICH) loading factors is studied. It is found that the best choice for the P-SCH loading factor is approximately 0.6–0.7 for the pipelined process considered, and the SCH loading factor should be no less than 10%. For capacity and acquisition time tradeoff, a good choice for the CPICH loading factor is in the range of 5% to 10%. Finally, a maximum likelihood based frequency estimation method based on despreading the CPICH signal, the Fast Fourier Transform, and a quadratic interpolation in the frequency domain is proposed. It is shown that this proposed method achieves more than 10 dB gain, compared to a differential detection scheme.

Acknowledgment

Many issues addressed in this paper were raised during numerous rounds of discussions in *Ad Hoc 12* of Working Group 1 (WG1), Technical Specification Group: Radio Access Network (TSG:RAN), 3rd Generation Partnership Project (3GPP). The authors acknowledge these fruitful discussions which improved our knowledge of the cell search problem. The most active members in *Ad Hoc 12* of 3GPP WG1 include colleagues from DoCoMo, Ericsson, Nokia, Nortel, Shinsegi, Siemens, and Texas Instruments. Also, the authors gratefully acknowledge Dr. Essam Sourour, Dr. Gregory E. Bottomley, and the anonymous reviewers of this paper for their helpful comments.

References

[1] T. Ojanperä and R. Prasad, "An overview of air interface multiple access for IMT-2000/UMTS," *IEEE Commun. Mag.*, vol. 36, pp. 82–95, Sept. 1998.

[2] E. Dahlman, P. Beming, J. Knutsson, F. Ovesjö, M. Persson, and C. Roobol, "WCDMA—The radio interface for future mobile multimedia communications," *IEEE Trans. Veh. Technol.*, vol. 47, pp. 1105–1118, Nov. 1998.

[3] 3rd Generation Partnership Project, "Spreading and modulation (FDD)," 3GPP Tech. Spec., TS 25.213, V3.0.0, Oct. 1999.

[4] R. L. Peterson, R. E. Ziemer, and D. E. Borth, *Introduction to Spread Spectrum Communication*. Englewood Cliffs, NJ: Prentice-Hall, 1995.

[5] K. Higuchi, M. Sawahashi, and F. Adachi, Fast cell search algorithm using long code masking in DS-CDMA asynchronous cellular system, Tech. Rep. IEICE, pp. 57–62, Jan. 1997.

[6] ——, "Fast cell search algorithm in DS-CDMA mobile using long spreading codes," in *Proc. IEEE 1997 Veh. Technol: Conf.*, Phoenix, AZ, May 1997, pp. 1430–1434.

[7] J. Nyström, K. Jamal, Y.-P. E. Wang, and R. Esmailzadeh, "Comparison of cell search methods for asynchronous wideband CDMA cellular system," in *Proc. IEEE 1998 Int. Conf. Universal Personal Commun.*, Florence, Italy, Oct. 1998.

[8] C. Östberg, Y.-P. E. Wang, and F. Jaenecke, "Performance and complexity of techniques for achieving fast sector identification in an asynchronous CDMA system," in *Proc. 1st Int. Symp. Wireless Personal Multimedia Commun.*, Japan, Nov. 1998, pp. 87–92.

[9] 3rd Generation Partnership Project, "Physical channels and mapping of transport channels onto physical channels (FDD)," 3GPP Tech. Spec., TS 25.211, V3.0.0, Oct. 1999.

[10] Siemens and Texas Instruments, "Generalized hierarchical Golay sequence for PSC with low complexity correlation using pruned efficient Golay correlators," 3GPP Tech. Doc., Tdoc R1-99554, Cheju, Korea, June 1999.

[11] S. Sriram and S. Hosur, "Fast acquisition method for DS-CDMA systems employing asynchronous base stations," in *Proc. IEEE Int. Conf. Commun.*, June 1999.

[12] 3rd Generation Partnership Project, "FDD: Physical layer procedures," 3GPP Tech. Spec., TS 25.214, V3.0.0, Oct. 1999.

[13] Y.-P. E. Wang and T. Ottosson, "Initial frequency acquisition in W-CDMA," in *Proc. IEEE Veh. Technol. Conf.*, Amsterdam, Sept. 1999, pp. 1013–1017.

[14] 3rd Generation Partnership Project, "UE radio transmission and reception (FDD)," TSG RAN WG4, version 3.0.0, Oct. 1999.

[15] D. C. Rife and R. R. Boorstyn, "Single tone parameter estimation from discrete-time observations," *IEEE Trans. Inform. Theory*, vol. IT-20, pp. 591–598, Sept. 1964.

[16] M. Luise and R. Reggiannini, "Carrier frequency recovery in all-digital modems for burst-mode transmissions," *IEEE Trans. Commun.*, vol. 43, pp. 1169–1177, Feb./Mar./Apr. 1995.

[17] U. Fawer, "A coherent spread-spectrum diversity-receiver with AFC for multipath fading channels," *IEEE Trans. Commun.*, vol. 42, pp. 1300–1311, Feb./Mar./Apr. 1994.

Yi-Pin Eric Wang (S'91–M'96) received the B.S. degree in electrical engineering from National Taiwan University in 1988, and the M.S. and Ph.D. degrees, both in electrical engineering, from the University of Michigan, Ann Arbor, in 1991 and 1995, respectively. He has been a member of the Advanced Development and Research group of Ericsson Inc. in Research Triangle Park, North Carolina, USA, since 1995. His work focuses on wireless communications, including mobile satellite communication systems and terrestrial cellular systems. His research interests include coding, modulation, synchronization, and interference cancellation in CDMA systems.

Tony Ottosson (S'93–M'98) was born in Uddevalla, Sweden, in 1969. He received the M.Sc. in electrical engineering from Chalmers University of Technology, Göteborg, Sweden, in 1993, and the Lic. Eng. and Ph.D. degrees from the Department of Information Theory, Chalmers University of Technology, in 1995 and 1997, respectively.

Currently he is an Associate Professor in the Communication Systems Group, Department of Signals and Systems, Chalmers University of Technology. During 1999 he was also working as a Research Consultant at Ericsson Inc., Research Triangle Park, NC, USA. From Oct. 1995 to Dec. 1998 he participated in the European FRAMES (Future Radio wideband Multiple Access System) project both as a Co-Worker and during 1998 as Activity Leader of the area of coding and modulation. His research interests are in communication systems and information theory and are mainly targeted to CDMA systems. Specific topics are modulation, coding, multirate schemes, multiuser detection, combined source-channel coding, joint decoding techniques and synchronization.